A simple biological imaging system for detecting viable human circulating tumor cells

Toru Kojima,[1,2] Yuuri Hashimoto,[1,3] Yuichi Watanabe,[1,3] Shunsuke Kagawa,[1,2] Futoshi Uno,[1,2] Shinji Kuroda,[1,2] Hiroshi Tazawa,[2] Satoru Kyo,[4] Hiroyuki Mizuguchi,[5] Yasuo Urata,[3] Noriaki Tanaka,[1] and Toshiyoshi Fujiwara[1,2]

[1]Division of Surgical Oncology, Department of Surgery, Okayama University Graduate School of Medicine, Dentistry and Pharmaceutical Sciences, Okayama, Japan. [2]Center for Gene and Cell Therapy, Okayama University Hospital, Okayama, Japan. [3]Oncolys BioPharma Inc., Tokyo, Japan. [4]Department of Obstetrics and Gynecology, Kanazawa University School of Medicine, Kanazawa, Japan. [5]Department of Biochemistry and Molecular Biology, Graduate School of Pharmaceutical Sciences, Osaka University, Osaka, Japan.

The presence of circulating tumor cells (CTCs) in the peripheral blood is associated with short survival, making the detection of CTCs clinically useful as a prognostic factor of disease outcome and/or a surrogate marker of treatment response. Recent technical advances in immunocytometric analysis and quantitative real-time PCR have made it possible to detect a few CTCs in the blood; however, there is no sensitive assay to specifically detect viable CTCs. Here, we report what we believe to be a new approach to visually detect live human CTCs among millions of peripheral blood leukocytes, using a telomerase-specific replication-selective adenovirus expressing GFP. First, we constructed a GFP-expressing attenuated adenovirus, in which the telomerase promoter regulates viral replication (OBP-401; TelomeScan). We then used OBP-401 to establish a simple ex vivo method that was able to detect viable human CTCs in the peripheral blood. The detection method involved a 3-step procedure, including the lysis of rbc, the subsequent addition of OBP-401 to the cell pellets, and an automated scan using fluorescence microscopy. OBP-401 infection increased the signal-to-background ratio as a tumor-specific probe, because the fluorescent signal was amplified only in viable, infected human tumor cells, by viral replication. This GFP-expressing virus-based method is remarkably simple and allows precise enumeration of CTCs.

Introduction

Determination of the extent of the disease is the most important factor in predicting the clinical outcome in cancer patients. Primary cancers have been known to shed tumor cells into the blood circulation, which represents the route for systemic tumor cell dissemination (1, 2). Indeed, the presence of circulating tumor cells (CTCs) in the peripheral blood is associated with short survival, and therefore the detection of CTCs is clinically useful as a prognostic factor of disease outcome and/or as a surrogate marker of treatment response (3, 4). Technical advances in immunocytometric analysis and quantitative real-time PCR have made it possible to detect a few CTCs in the blood; however, background expression of cancer-associated antigens, such as cytokeratin 8 (CK-8), CK-18, and CK-19, in normal epithelial cells results in the false-positive detection, and PCR-based methods can not permit analysis of cell morphology. Moreover, there is no sensitive assay for detecting viable CTCs.

The GFP, which was originally identified from the jellyfish *Aequorea victoria*, is an attractive molecular marker for imaging in live tissues because of the relatively noninvasive nature of fluorescent (5–8). It has been reported that hormone-refractory human prostate carcinoma, growing orthotopically in nude mice, efficiently deliver viable tumor cells in the host circulation, which could be detectable using the fluorescence microscopy, when marked by GFP expression (9). In addition, isolated rare CTCs showed an increased metastatic propensity. We reported previously that intratumoral injection of telomerase-specific replication-selective adenovirus expressing the *gfp* gene (OBP-401; TelomeScan) causes viral spread into the regional lymphatics, with subsequent selective replication in neoplastic lesions, resulting in GFP expression in metastatic lymph nodes in *nu/nu* mice (10). The present study extended our previous work, by developing what we believe to be a novel and simple strategy to selectively label human CTCs with fluorescence among millions of peripheral blood leukocytes. The detection method involves 3-steps: the lysis of rbc, the subsequent addition of OBP-401 to the cell pellets, and the automated scan under the fluorescence microscope. This method allows precise enumeration of human CTCs, because OBP-401 can replicate and express GFP fluorescence only in viable tumor cells.

Results

Selective GFP expression in human cancer cells in vitro by OBP-401. OBP-401 (TelomeScan) was constructed by inserting the *gfp* gene under the control of the CMV promoter at the deleted E3 region of the telomerase-specific replication-selective type 5 adenovirus OBP-301 (Telomelysin) (11, 12) (Figure 1). To determine whether telomerase activity is associated with selective GFP expression in different cancer cell lines, we measured human telomerase reverse transcriptase (*hTERT*) mRNA and GFP expression using quantitative real-time RT-PCR analysis and fluorescence microplate reader, respectively. The *hTERT* expression was directly proportional to the fluorescence intensity, and regression analysis confirmed a strong correlation between these numbers ($r^2 > 0.94$) (Figure 1B). H1299 human non–small cell lung cancer cells expressed bright GFP fluorescence as early as 12 hours after OBP-401 infection, and a positive signal for GFP was detected in all cells at 48 hours after infec-

Conflict of interest: Yasuo Urata is an employee of Oncolys BioPharma Inc., the manufacturer of OBP-401 (TelomeScan).

Citation for this article: *J. Clin. Invest.* **119**:3172–3181 (2009). doi:10.1172/JCI38609.

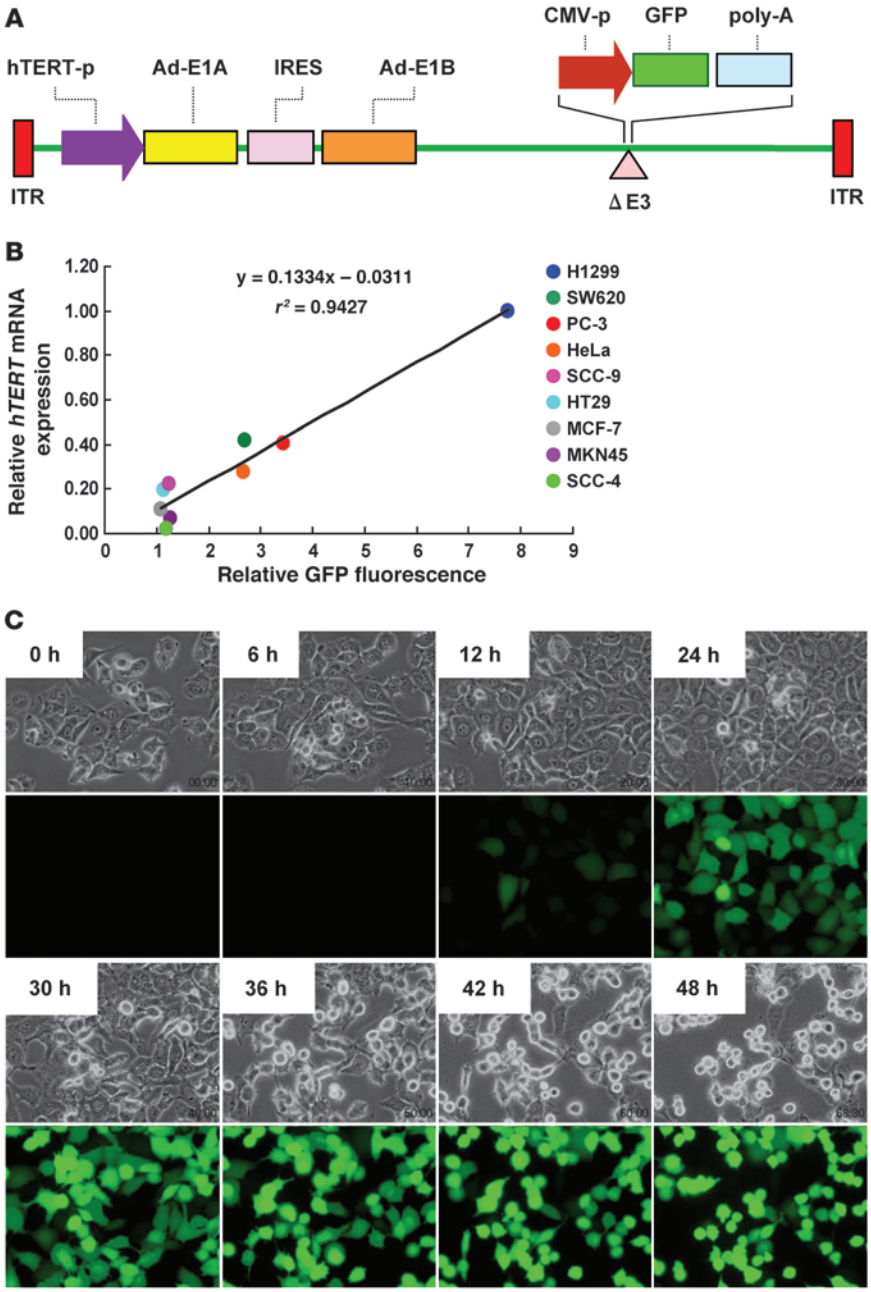

Figure 1
Schematic DNA structure of OBP-401 and selective replication of OBP-401 in human cancer cells. (**A**) OBP-401 is a telomerase-specific replication-competent adenovirus variant, in which the hTERT promoter element drives expression of the *E1A* and *E1B* genes linked with an IRES, and the *gfp* gene is inserted under the CMV promoter into the E3 region for monitoring viral replication. hTERT-p, hTERT promoter; Ad-E1A, adenoviral E1A; Ad-E1B, adenoviral E1B; CMV-p, CMV promoter; poly-A, polyadenylation signal; ITR, inverted terminal repeat. (**B**) Relationship between *hTERT* expression and GFP fluorescence. Relative *hTERT* mRNA expression and GFP fluorescence in human tumor cell lines were determined by real-time RT-PCR analysis and fluorescence microplate reader, respectively. The relative *hTERT* mRNA expression ratios normalized by dividing the value of H1299 cells are presented for each sample. Relative GFP fluorescence was measured 48 hours after OBP-401 infection at an MOI of 10. (**C**) Time-lapse images of H1299 human lung cancer cells were recorded for 48 hours after OBP-401 infection at an MOI of 10. Selected images taken at the indicated time points show cell morphology by phase-contrast microscopy (top panels) and GFP expression under fluorescence microscopy (bottom panels). Original magnification, ×200.

tion (Figure 1C and Supplemental Video 1; supplemental material available online with this article; doi:10.1172/JCI38609DS1). OBP-401 infection also induced GFP expression in other neoplastic cells such as human sarcoma cell lines within 24 hours after infection (Supplemental Figure 1 and Supplemental Video 2). In parallel experiments, OBP-401 infection induced dose-dependent GFP expression in a variety of human cancer cell lines that originated from different organs (Supplemental Figure 2).

Measurement of viable CTCs with OBP-401 in the blood. We used OBP-401 to establish a simple ex vivo method for detecting viable human CTCs in the peripheral blood. As illustrated in Figure 2A, the method involves a 3-step procedure, including the lysis of rbc in 5-ml aliquots of whole blood samples, subsequent addition of 10^4 PFUs of OBP-401 to the cell pellets, and the deposition of cells on polylysine-coated slides, followed by automated scanning under a fluorescence microscope. OBP-401 infection increases the signal-to-background ratio as a tumor-specific probe, because the fluorescent signal can be amplified only in tumor cells by telomerase-specific viral replication. The automated optical scan system provides high speed and accuracy of slide movement in all x, y, and z directions for the acquisition of a large number of high-resolution segmented tile images, at a magnification of ×100 for each tile (Figure 2B). Each optical field is focused automatically before image acquisition. The captured segmented tile images are automatically combined to construct a large image, with a total area of 20 × 20 mm. Since each tile segment can be magnified without the loss of high resolution, OBP-401–infected human tumor cells could be easily visualized with GFP signals in blood smears (Figure

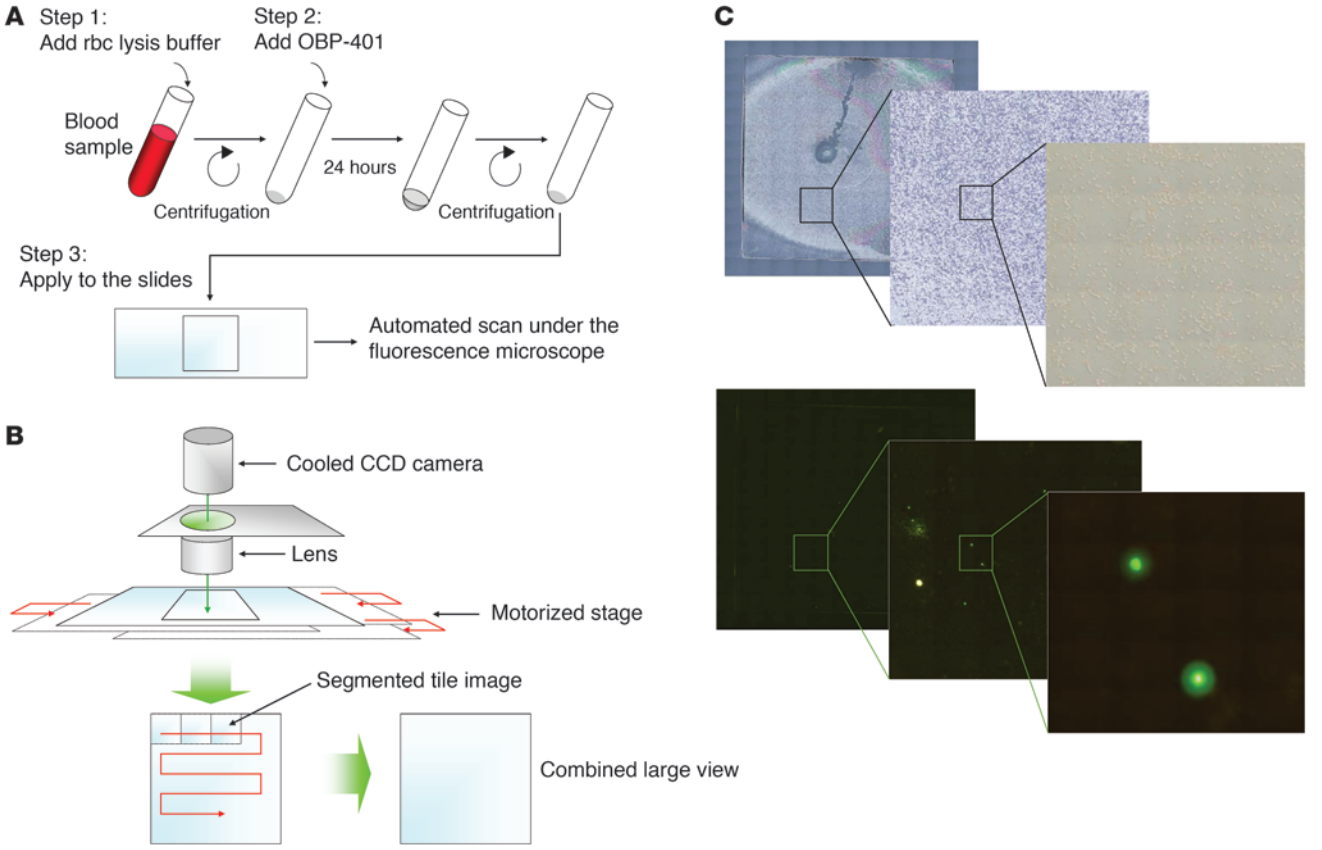

Figure 2

A simple method to detect telomerase-positive cells in the blood. (**A**) Steps in the sample preparation for GFP fluorescence detection. Blood samples (5-ml samples) are collected in heparinized tubes and incubated with rbc lysis buffer containing ammonium chloride (NH_4Cl) for 15 minutes. After centrifugation, cell pellets are mixed with 10^4 PFUs of OBP-401 and incubated at room temperature for another 24 hours. Cells are resuspended in 15 μl of PBS following centrifugation and then placed onto the slide under a coverslip. (**B**) System for automated fluorescence molecular imaging. The automated optical scan system serially captures segmented tile images in the area of the coverslip under fluorescence microscopy. (**C**) A high-resolution large view of the reconstructed tile images. The zoomed image allows easy visualization of GFP-expressing cells among millions of blood leukocytes. Original magnification, ×40 (left panels); ×100 (middle panels); ×400 (right panels).

2C). This automated microscopic scan system allows us to obtain high-magnification images with a large field of view.

Accuracy of CTC detection by ex vivo OBP-401 infection. To test the efficacy and accuracy of the system, whole blood samples from healthy donors were spiked with variable numbers of H1299 human lung cancer cells and then analyzed. Representative images of each sample are shown in Figure 3A. H1299 cells could be distinguished from the other blood cells even at lower magnification. The recovery of tumor cells was consistent over a target frequency range, between 10 and 1,000 cells spiked into 5 ml of blood from normal donors. Regression analysis of the number of GFP-positive cells versus the number of expected tumor cells yielded a correlation coefficient of $r^2 = 0.9996$ (Figure 3B). Thus, the number of GFP-positive cells reflects the actual peripheral blood tumor cell load. We also performed immunohistochemical analysis with anti-human CK-7/8 antibody to ensure that the cells labeled with GFP signals were indeed tumor cells. We used CK-7/8 as a marker for tumor cell detection, as H1299 cells were completely negative for CK-19 (Supplemental Figure 3). The automated microscopic scan system permits repeated scanning of the same fields repeatedly by a 2-dimensional line scanning technology. Merged images of fluorescent detection and CK-7/8 immunostaining confirmed that H1299 human lung cancer cells stably transfected with the *gfp* gene were CK-7/8 positive in the blood smear (Supplemental Figure 3). By using this dual imaging method, we confirmed that the GFP-positive cells were CK-7/8 positive following 24-hour exposure to OBP-401 and were distinguishable from other blood cells (Figure 3C). GFP-expressing cells were also morphologically classified as tumor cells (data not shown).

Comparative analysis of CTC detection by OBP-401, real-time RT-PCR, and flow cytometry. To compare the GFP-based CTC detection and other existing methods, blood samples spiked with variable numbers of H1299 cells were also analyzed. We performed real-time RT-PCR analysis with primers targeting the *hTERT* gene, as OBP-401–mediated GFP expression reflects the telomerase activity (Figure 1B). The number of GFP-positive cells was proportional to the increasing number of H1299 cells, between 10 and 1,000 cells in 5 ml of blood after ex vivo OBP-401 infection (Figure 3B); a significant increase in amplification, however, could not be observed even with 2,000 tumor cells in 1 ml of blood by real-time RT-PCR (Figure 4A), suggesting that the detected *hTERT* mRNA levels might be the background expression. In addition, a

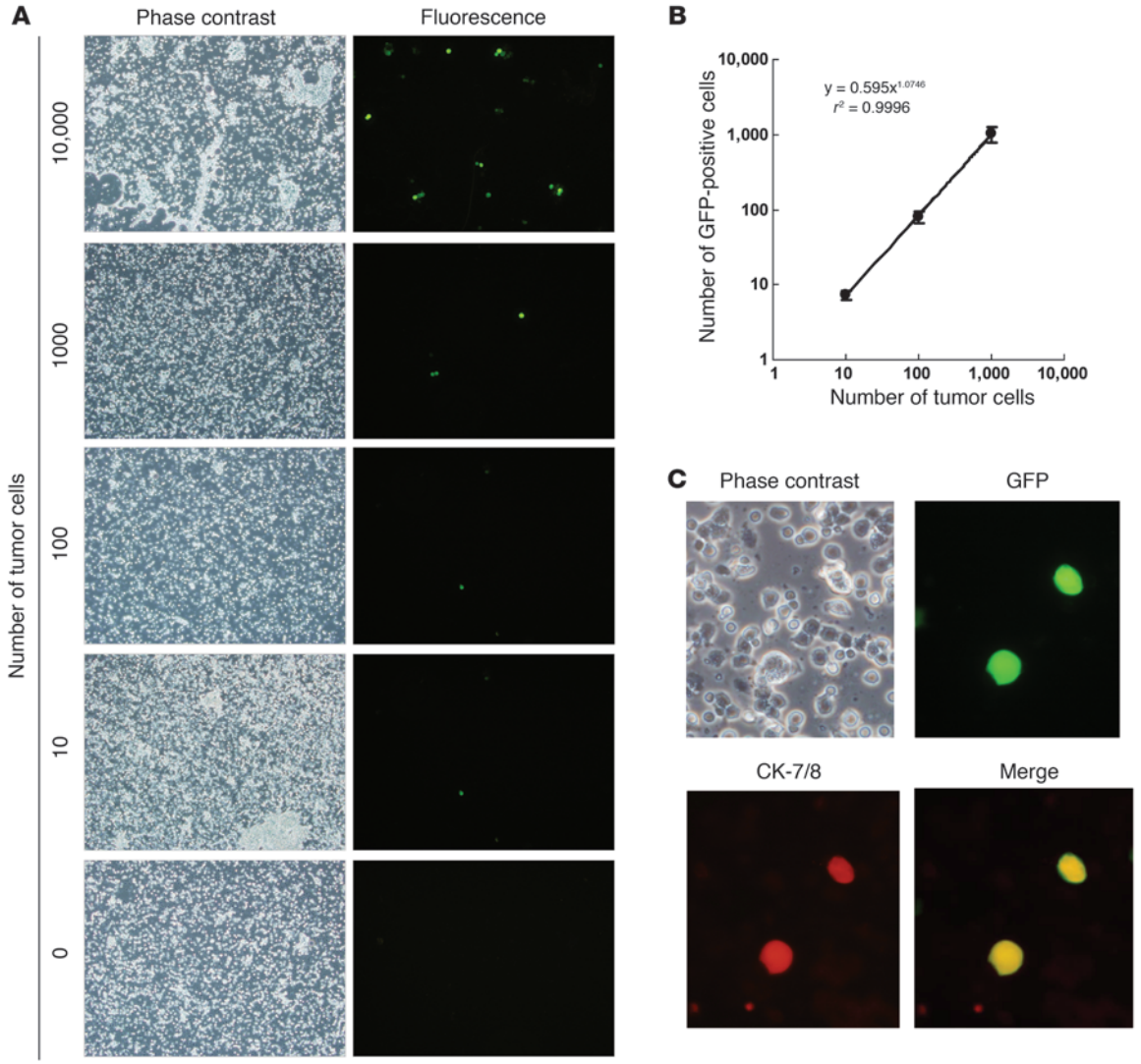

Figure 3
Selective visualization of human cancer cells by OBP-401. (**A**) Phase-contrast and fluorescent images of peripheral blood cells mixed with H1299 human lung cancer cells. Variable numbers of H1299 cells were spiked into 5 ml of whole blood samples from healthy donors and then immediately analyzed for GFP expression. Original magnification, ×100. (**B**) Efficiency of labeling tumor cells added to whole human blood with OBP-401. The number of tumor cells spiked into whole blood versus the number of GFP-expressing cells is plotted. Each value represents the mean ± SD. (**C**) Immunohistochemical staining of GFP-expressing cells for CK-7/8. The blood samples mixed with H1299 cells were analyzed for GFP expression, fixed with 2% glutaraldehyde, and then stained with rhodamine-labeled anti–CK-7/8 antibody. Overlap of green (GFP) and red (CK-7/8) fluorescence was displayed as yellow fluorescence. Original magnification, ×600.

quantitative RT-PCR assay could not detect *CK7* mRNA expression in all samples tested (Figure 4B), although H1299 cells were positive for CK-7/8 (Supplemental Figure 4). We also used flow cytometry to detect H1299 tumor cells in the blood; however, the number of GFP-positive cells following ex vivo OBP-401 infection was much lower than expected (Supplemental Figure 4 and Figure 4C). These results suggest that enrichment of tumor cells or depletion of unwanted cells is necessary for CTC detection by real-time RT-PCR and flow cytometry.

Viable CTCs detected with OBP-401 in patients with various cancers. To examine whether CTCs from cancer patients can be labeled with GFP signals by OBP-401 replication to permit their detection in whole blood, we analyzed fresh blood samples collected from 37 patients with histologically confirmed gastric cancer and 9 patients with other malignancies, including colon cancer, hepatocellular carcinoma (HCC), breast cancer, and non–small cell lung cancer. Although the CTC level varied widely, ranging from 0 to 47 cells in 5-ml samples, 26 gastric cancer patients (70.3%) had more than 1 CTC; there was, however, no apparent relationship between CTC counts and TNM stages (Figure 5A, Table 1, and Supplemental Table 1). CTCs were also identified in samples from 6 of 9 (66.7%) patients with other cancers. The number of CTCs that were isolated ranged from 0 to 56 cells per 5-ml sample (Figure 5B, Table 1, and Supplemental Table 2).

To confirm the infectivity of OBP-401 to tumor cells at the primary sites, we applied this assay to single-cell suspensions isolated

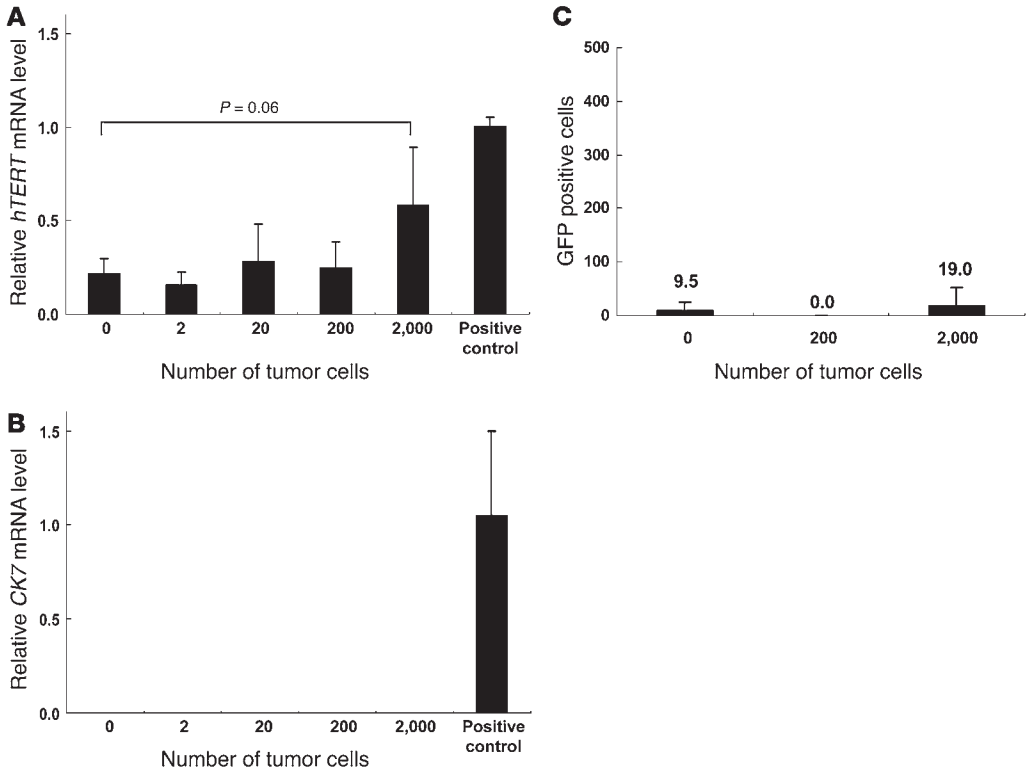

Figure 4

Comparison of the sensitivity of CTC detection by real-time RT-PCR and flow cytometry. (**A** and **B**) Variable numbers of H1299 cells spiked into 1 ml of whole blood samples from healthy donors were prepared. The relative expression of *hTERT* (**A**) and *CK7* (**B**) mRNA was determined by real-time RT-PCR analysis. The amount of *hTERT* and *CK7* mRNA was normalized with data from the real-time amplification of the *GAPDH* housekeeping gene. The blood without H1299 cells was used as a negative control, and H1299 cells without the blood were used as a positive control. (**C**) Flow-cytometric enumeration of variable numbers of H1299 cells mixed in 1 ml of blood samples. After the lysis of rbc, blood samples were infected with 10^4 PFUs of OBP-401 for 24 hours, and then subjected to flow-cytometric analysis. The numbers above the bars indicate the actual numbers of GFP-positive cells. Each value represents the mean ± SD of triplicate experiments.

from surgically removed primary tumors. A gallery of cellular images showed sufficient GFP expression in tumor cells obtained from gastric and colon cancer patients, following OBP-401 infection at a MOI of 100 (Figure 6). The size and morphology of GFP-labeled cells isolated from primary tumors were consistent with those of CTCs detected in the peripheral blood of the same patients.

We further assessed the CTC dynamics in patients who were undergoing chemotherapy or surgery, to demonstrate the clinical potential of our approach for monitoring treatment responses. The results from a representative patient with advanced stage IV gastric cancer (case 1) are shown in Figure 7A. A 5-ml blood sample contained 6 CTCs before treatment. Fourteen days after the initiation of systemic chemotherapy, 7 CTCs were detected in the peripheral blood; the patient, however, had no CTCs after 2 cycles of chemotherapy. A patient who had a recurrence of gastric cancer in the regional lymph nodes (case 10) had decreased CTC counts after a cycle of chemotherapy (Figure 7B). Elimination or reduction of CTCs correlated well with a decrease in the levels of tumor markers such as CEA, CA19-9, and CA125. In contrast, the number of CTCs gradually increased in an advanced gastric cancer patient (case 25) who developed retroperitoneal tumor invasion despite chemotherapy (data not shown). As this patient showed no elevated levels of tumor markers, the kinetic of CTC numbers would enable a faster prediction of the treatment response than that of other radiographic imaging methods. In the 4 patients who underwent surgery (gastric cancer, cases 5 and 9; colon cancer, cases 3 and 4), the CTC level dropped 4 weeks after complete resection (Figure 7, C and D). These results suggest that enumeration of CTCs might be useful for monitoring the efficacy of local and systemic treatments.

Discussion

Early and accurate evaluation of therapeutic efficacy is the hallmark of successful cancer treatment. We have described a simple method, without any complicated processing steps, for detecting viable human CTCs in the peripheral blood, by using telomerase-specific GFP-expressing adenovirus. Viable CTCs may be a less-invasive, repeatable biomarker for monitoring tumor responses against various types of therapies, although its clinical significance is still debatable. In our pilot study, reported herein, serial blood sampling demonstrated that surgical removal of primary tumors was associated with decreased CTC counts. Thus, quantitative detection of CTCs can be also a substantial surrogate marker for treatment efficacy in candidates for chemotherapy.

The technical platform of CTC enumeration has improved rapidly (13). PCR-based techniques, which are commonly used to detect CTCs (14, 15), can detect dead tumor cells and cell-free circulating DNA or RNA, which may result in overestimation of the neoplastic

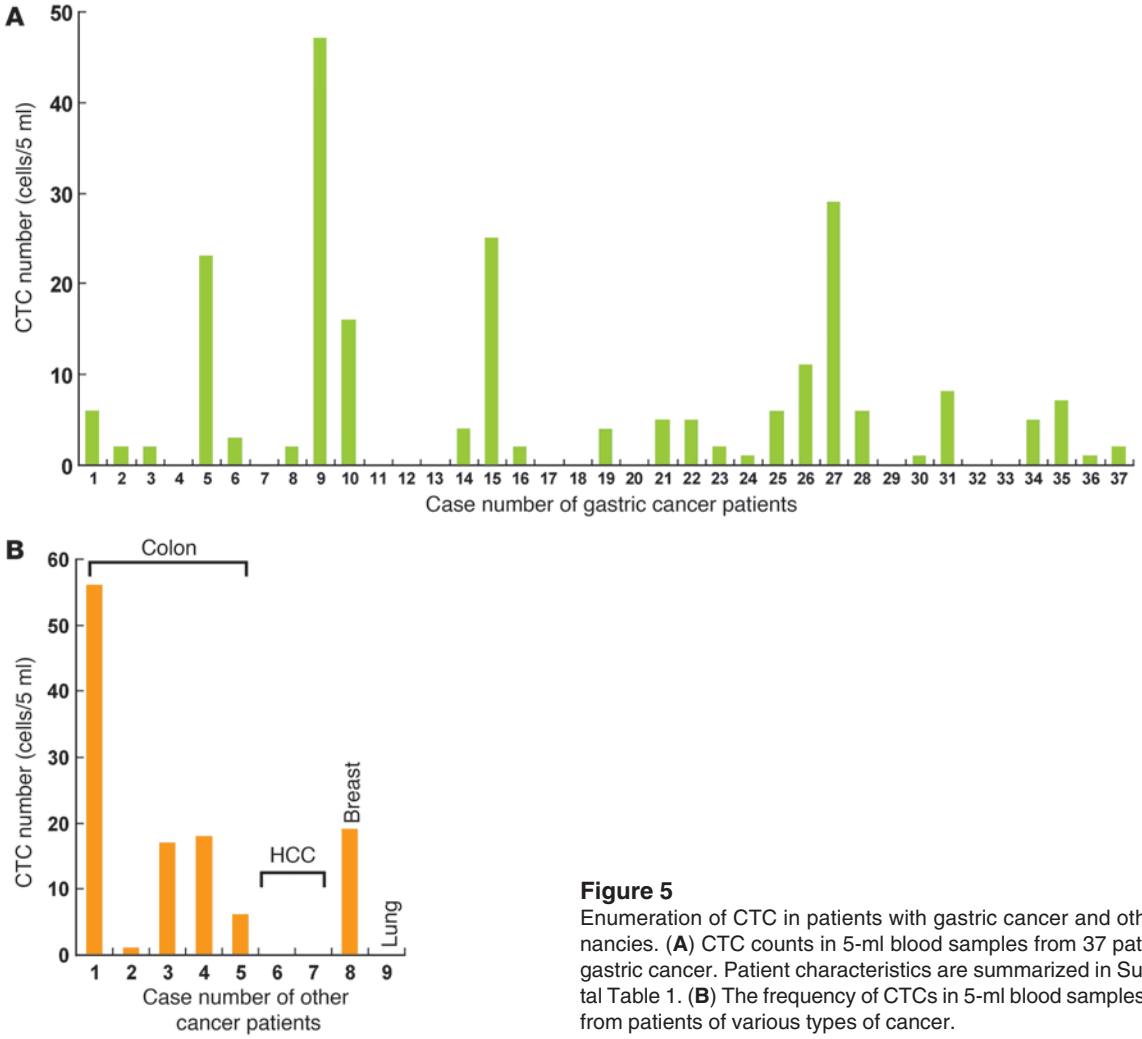

Figure 5
Enumeration of CTC in patients with gastric cancer and other malignancies. (**A**) CTC counts in 5-ml blood samples from 37 patients with gastric cancer. Patient characteristics are summarized in Supplemental Table 1. (**B**) The frequency of CTCs in 5-ml blood samples obtained from patients of various types of cancer.

state. In addition, our data demonstrated that neither quantitative RT-PCR for *hTERT* mRNA nor that for *CK7* mRNA could identify as many as 2,000 human tumor cells per 1 ml of blood without enrichment. Recently, Diehl et al. have reported that circulating tumor DNA is useful as a measure of tumor dynamics and that it can be beneficial for monitoring many types of human cancer (16). Although the system has the ability to quantify the level of circulating DNA and the sufficient sensitivity to detect very small amount of nucleic acids, it requires the identification of a somatic mutation in the individual tumor by sequencing of DNA. Our GFP-based fluorescence imaging can allow simple detection of target cancer cells, without any time-consuming steps, and it seems to be much more reliable and sensitive.

To date, various approaches have been also used to visually identify CTCs; however, the techniques employed to perform cell enrichment, immunohistochemical detection, and image analysis are complicated (17–19). Moreover, epithelial markers are currently used to detect CTCs; tumor cells, however, may lose their epithelial features during metastasis/dissemination or may not express these markers because of their heterogeneity (20). Indeed, the human non–small cell lung cancer cells that we used lack CK-19 expression, which is the marker most extensively studied for the detection of CTCs. The mechanism by which epithelial cells acquire the motile properties is epithelial-to-mesenchymal transition (EMT), a process that is currently popular for investigators of the onset of cancer cell migration, invasion, and metastatic dissemination (21, 22). EMT also promotes cytoskeletal rearrangement in tumor cells, which results in the downregulation of epithelial markers and upregulation of mesenchymal markers (22, 23). Nagrath et al. developed a unique microfluidic platform (CTC-chip) for CTC separation by using anti–epithelial cell adhesion molecule (EpCAM) antibody, and they demonstrated sensitive real-time monitoring of responses to cancer therapy with this technology (24); the loss of EpCAM expression, however, has been reported in metastatic and drug-resistant cancer cells (25). The multimarker assay may show slightly increased sensitivity for CTC detection over the single-marker method (26, 27); the procedures, however, are complicated. In contrast, telomerase is activated in most human cancers and is known to be associated with their malignant properties (28). Recent studies have reported that EMT can produce the cancer stem cell phenotype (29, 30). Since telomerase activity is one of the stem-cell properties (31), our system may be capable of detecting circulating cancer stem cells, even with EMT features, such as the loss and/or redistribution of the epithelial markers, that are

Table 1
CTC numbers classified by disease stage (as defined by the TNM classification system) and type

Cancer	Stage	GFP-positive cells (per 5 ml)					
		0	1–5	6–10	11–20	21–30	≥31
Gastric	I	5	5	2			1
Gastric	II		4			2	
Gastric	III	3	2	1			
Gastric	IV	3	4	1	2	1	
Colon	I				1		
Colon	II						
Colon	III			1	1		1
Colon	IV		1				
HCC	II	1					
HCC	III	1					
Breast	IV				1		
Lung	I	1					

responsible for metastasis. Moreover, as GFP-positive cells could be collected by flow-cytometric sorting (32), this technology might be applicable for molecular analysis of CTCs.

One of the crucial features that we believe to be unique of our approach is to use the virus with the self-proliferation potency. Although adenovirus-mediated transduction of the reporter genes into target cells is a common strategy in basic research, to the best of our knowledge, this is the first demonstration of ex vivo visualization of live CTCs, with a genetically engineered adenoviral agent, combined with an automated optical scan system for clinical studies. Infection efficiency of the adenoviral agent, which is derived from human adenovirus serotype 5, varies widely depending on the expression of Coxsackie-adenovirus receptor (CAR) (33). This might be one of the potential advantages of our system, because most of human hematopoietic cells are almost refractory to transduction by adenovirus vectors, due to the lack of CAR for virus binding (34). Therefore, when OBP-401 is used to detect CTCs in the peripheral blood, OBP-401 infection is limited in hematopoietic cells, including leukocytes. Moreover, OBP-401 replication is unlikely in normal hematopoietic cells, because of their low telomerase activity.

Our patient data demonstrate that enumeration of CTCs reflects the tumor burden, as the CTC counts decreased upon complete surgical removal of primary tumors. In addition, although the sample size is too small to perform a statistical analysis, 2 gastric cancer patients, who favorably responded to systemic chemotherapy, exhibited a gradual lowering of CTC counts in parallel with a decrease in the level of tumor markers, whereas a radiographically nonresponding patient had an increased CTC count. In contrast, the absolute number of CTCs did not correspond with tumor sizes or TNM stages in patients, and a small number of CTCs (0–4 cells in 5-ml samples) were detected in healthy normal volunteers (data not shown). These results suggest that it is more important to measure the change in CTC quantity, than to simply determine whether the value is below or above a disease-specific cutoff point; the CTC count was, however, mostly analyzed with this endpoint in clinical trials that used immunomagnetic-bead purification (3, 4, 17). Recently, Scher et al. have demonstrated that the use of CTC count as a continuous variable enables the prediction of survival in patients with castration-resistant prostate cancer (35). Although we cannot comment on the prognostic utility of CTC values in the absence of outcome data, our OBP-401–based method is at least useful as a measure of tumor dynamics. A larger series of clinical trials and longer follow-up studies are necessary to confirm the feasibility of this technology.

In conclusion, we developed an ex vivo GFP-based fluorescence imaging system that is very simple and suitable for accurate identification and enumeration of viable CTCs. This technology has the potential to allow physicians to assess the response to treatment as a relevant clinical parameter, especially in patients without elevated levels of tumor markers.

Methods

Cell culture. The human non–small cell lung cancer cell line H1299, the human tongue squamous carcinoma cell lines SCC-4 and SCC-9, the human gastric cancer cell line MKN45, the human colorectal cancer cell lines HT-29 and SW620, the human prostate cancer cell line PC-3, the human cervical adenocarcinoma cell line HeLa, and the human mammary gland adenocarcinoma cell line MCF-7 were cultured according to the specifications supplied by the vendor.

Virus. OBP-401 is a telomerase-specific replication-competent adenovirus variant, in which the hTERT promoter element drives the expression of the *E1A* and *E1B* genes linked with an internal ribosome entry site (IRES), and the *gfp* gene is inserted under the CMV promoter into the E3 region (7, 8, 10). The virus was purified by ultracentrifugation in cesium chloride step gradients, the titer was determined by a plaque-forming assay using 293 cells, and the virus sample was stored at –80°C.

Quantitative real-time RT-PCR analysis. Total RNA from cultured cells was obtained by using the RNeasy Mini Kit (Qiagen). The *hTERT* and *CK7* mRNA copy numbers were determined by real-time quantitative RT-PCR with a StepOnePlus system and TaqMan Gene Expression Assays (Applied Biosystems). Specific primers for hTERT (Hs00972650_m1), CK-7 (Hs00559840_m1), and GAPDH (Hs99999905_m1) were used (Applied Biosystems). PCR amplification began with a 20-second denaturation step at 95°C and then 40 cycles of denaturation at 95°C for 1 second and annealing/extension at 60°C for 20 seconds. Data analysis was performed using StepOne Software (Applied Biosystems). The *GAPDH* housekeeping gene was used as the reference gene for PCR normalization. The ratios normalized by dividing the value of H1299 cells were presented for each sample.

Fluorescence microplate reader. Cells were infected with OBP-401 at the indicated MOI values in a 96-well black-bottom culture plate and then further incubated for the indicated time periods. GFP fluorescence was measured by using a fluorescence microplate reader (DS Pharma Biomedical) with excitation/emission at 485 nm/528 nm. The GFP fluorescence was expressed relative to that of MCF-7 cells.

Time-lapse fluorescence microscopy. Cells were infected with OBP-401 at an MOI of 10 for 2 hours in vitro. Phase-contrast and fluorescent time-lapse recordings were obtained to concomitantly analyze cell morphology and GFP expression with an inverted microscope (Olympus) equipped with a heated stage and controlled CO_2 environment (37°C, 8.5% CO_2) (Tokai Hit). Images were taken every 10 minutes.

Sample preparation and automated optical imaging analysis. A simple 3-step method is used to detect viable human CTCs in the peripheral blood. Briefly, 5-ml blood samples were drawn into heparinized tubes and incubated with lysis buffer containing ammonium chloride (NH_4Cl) for 15 minutes to remove

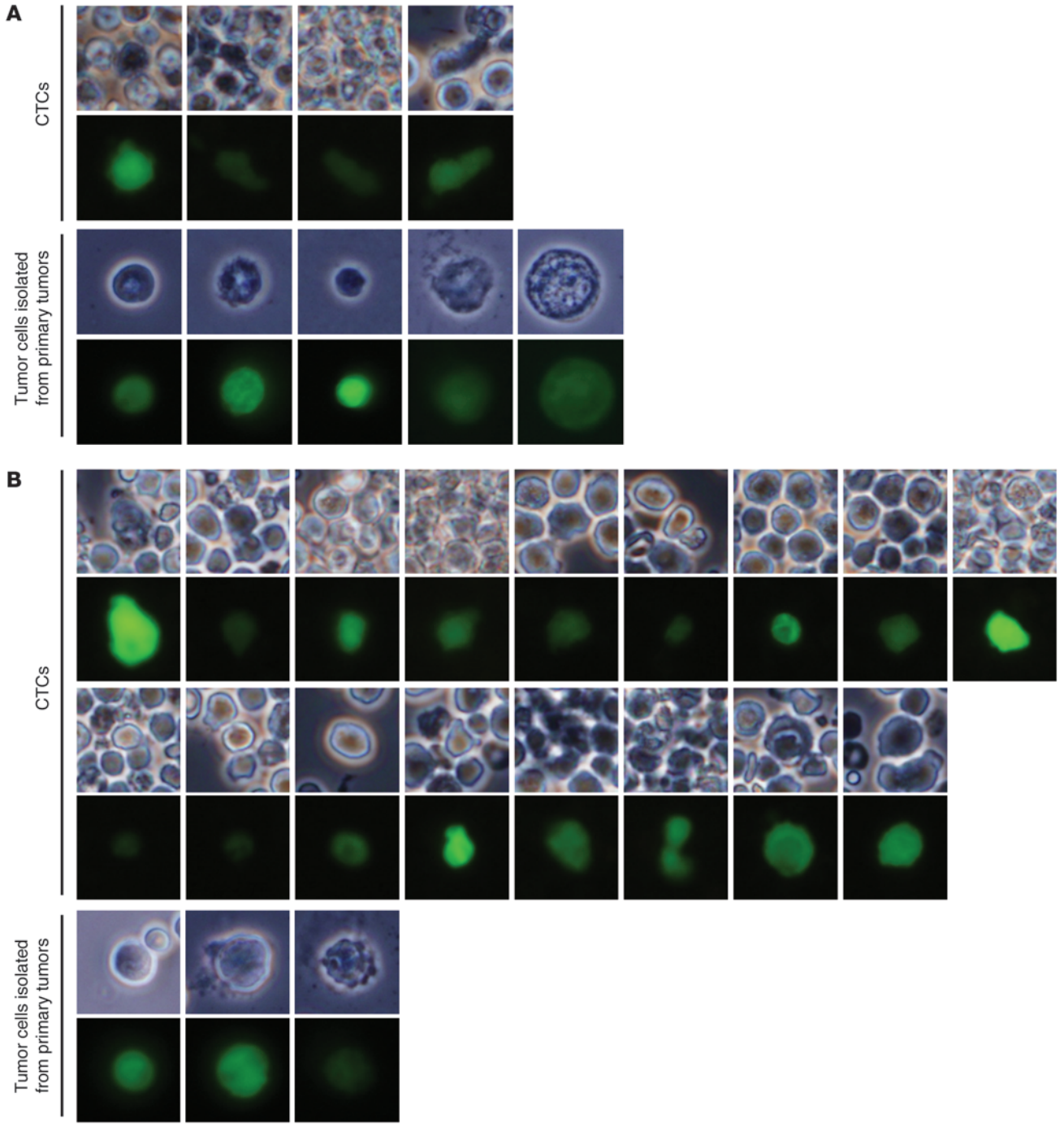

Figure 6
Images of GFP-positive cells obtained from the peripheral blood and the primary tumors. (**A**) CTCs were visualized by GFP expression among peripheral blood leukocytes in the blood sample obtained from a stage Ib gastric cancer patient (case 31). A single-cell suspension was also prepared from surgically removed primary tumor and exposed to OBP-401 at an MOI of 100 for 24 hours. (**B**) Primary tumor cells were also isolated from a patient with stage IIIa colon cancer (case 3) and infected with OBP-401 at an MOI of 100. Cell morphology of CTCs and primary tumor cells is shown by phase-contrast microscopy (first and third rows in **A** and first, third, and fifth rows in **B**), and GFP expression is shown by fluorescence microscopy (second and fourth rows in **A** and second, fourth, and sixth rows in **B**). Original magnification, ×600.

erythrocytes. After centrifugation, the cell pellets were mixed with 10^4 PFUs of OBP-401 and incubated at room temperature for another 24 hours. Following centrifugation, the cells were resuspended in 15 μl of PBS and then placed onto a slide under a coverslip. A motorized stage (Tokai Hit), mounted on a fluorescence microscope, serially captured segmented tile images in the area of the coverslip. The captured segmented tile images were joined together by MetaMorph 7.5, an image acquisition and analysis software (Molecular Devices), to create a large image of a 20-mm × 20-mm area. GFP signals could be

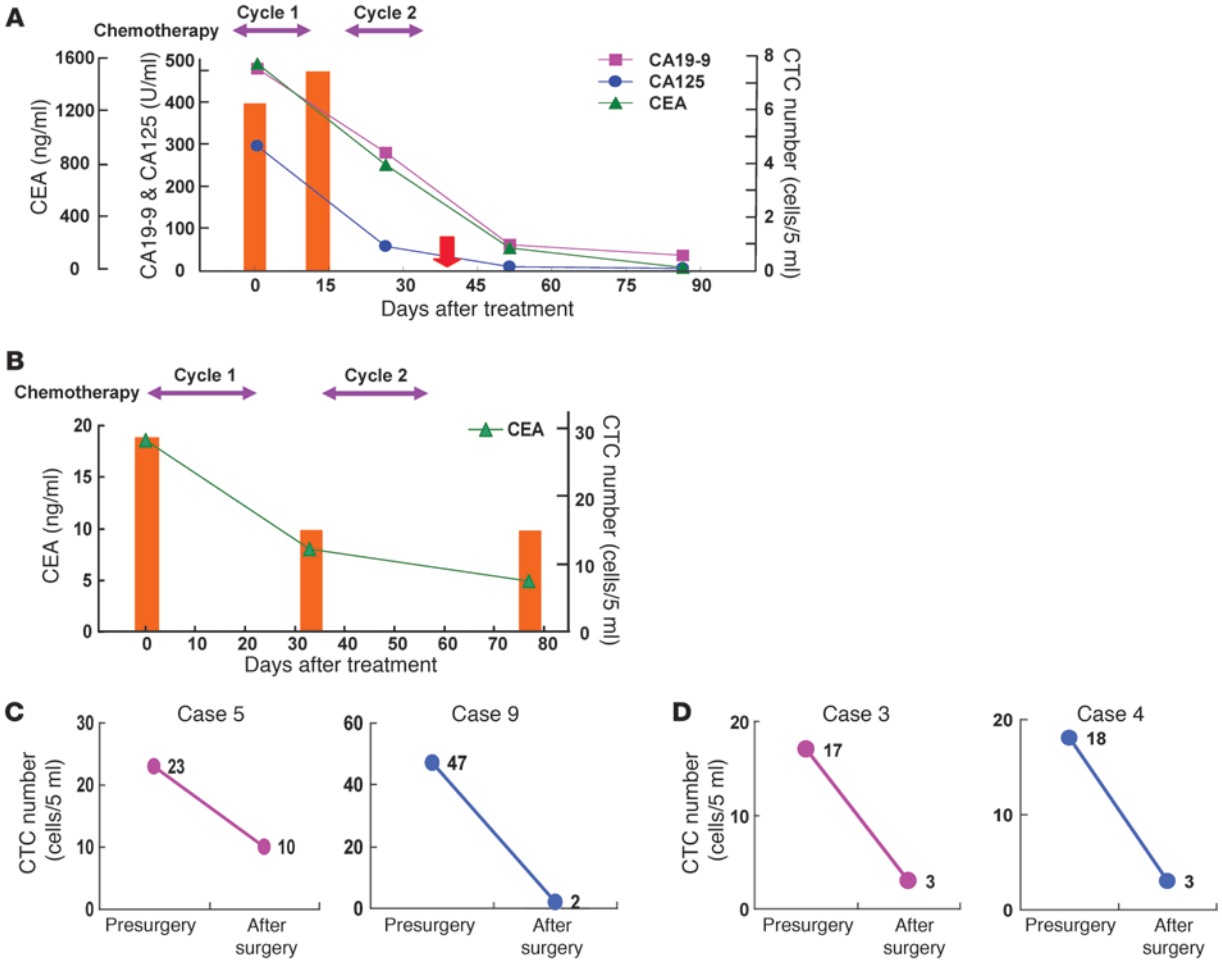

Figure 7

CTC dynamics at baseline and after treatment in patients with gastric or colon cancer. (**A**) Quantitation of CTCs in peripheral blood samples from an advanced gastric cancer patient (case 1) with multiple liver metastases who received 2 cycles of systemic chemotherapy. CTC counts at the indicated time points (orange bars) were plotted along with the levels of tumor markers CEA, CA19-9, and CA125. A decrease in the CTC number from 7 to 0 was observed 38 days after starting chemotherapy (red arrows). (**B**) The patient with recurrent gastric cancer at regional lymph nodes (case 27) was treated with 2 cycles of systemic chemotherapy. The CTC quantity (orange bars) and CEA level were well correlated over the course of treatment. (**C** and **D**) Changes in CTC numbers after surgery. CTC numbers were measured before and 4 weeks after surgical resection of primary tumors and regional lymph node dissection. (**C**) Two gastric cancer patients (cases 5 and 9) underwent a total gastrectomy and distal gastrectomy, respectively. (**D**) Low anterior resection was performed in 2 colorectal cancer patients (cases 3 and 4).

visualized easily in high-magnification images with a large field of view. The institutional review board at Okayama University Graduate School approved the study protocol, and all patients provided written informed consent.

Immunohistochemistry. Cells on the slides were fixed with 2% glutaraldehyde and washed 3 times with PBS. The slides were subsequently incubated with rhodamine-labeled anti–CK-7/8 antibody (CAM5.2; BD Biosciences) for 1 hour at 37°C. After washing 3 times with PBS, the slides were mounted with buffered glycerol for examination by fluorescence microscopy.

Tumor cell preparation. Primary solid tumors were surgically removed from patients with gastric cancer or other types of cancer. The tumor tissue was homogenized by mechanical mincing, and then the cell mixtures were passed through a cell strainer (BD Biosciences — Discovery Labware) and suspended as a single-cell suspension.

Statistics. We used the Student's 2-tailed *t* test to identify statistically significant differences between groups. Results are reported as mean ± SD. *P* values of less than 0.05 were considered statistically significant.

Acknowledgments

We thank Daiju Ichimaru and Hitoshi Kawamura for their helpful discussions. We also thank Tomoko Sueishi, Mitsuko Yokota, and Noriko Imagawa for their excellent technical supports. More importantly, we thank all participated patients for their courage and cooperation. This work was supported by Grants-in-Aid from the Ministry of Education, Science, and Culture, Japan and grants from the Ministry of Health and Welfare, Japan.

Received for publication January 16, 2009, and accepted in revised form July 1, 2009.

Address correspondence to: Toshiyoshi Fujiwara, Center for Gene and Cell Therapy, Okayama University Hospital, 2-5-1 Shikata-cho, Okayama 700-8558, Japan. Phone: 81-86-235-7997; Fax: 81-86-235-7884; E-mail: toshi_f@md.okayama-u.ac.jp.

1. Fidler, I.J. 1973. The relationship of embolic homogeneity, number, size and viability to the incidence of experimental metastasis. *Eur. J. Cancer.* **9**:223–227.
2. Liotta, L.A., Kleinerman, J., and Saidel, G.M. 1974. Quantitative relationships of intravascular tumor cells, tumor vessels, and pulmonary metastases following tumor implantation. *Cancer Res.* **34**:997–1004.
3. Cristofanilli, M., et al. 2004. Circulating tumor cells, disease progression, and survival in metastatic breast cancer. *N. Engl. J. Med.* **351**:781–791.
4. Cristofanilli, M., et al. 2005. Circulating tumor cells: a novel prognostic factor for newly diagnosed metastatic breast cancer. *J. Clin. Oncol.* **23**:1420–1430.
5. Hoffman, R.M. 2005. The multiple uses of fluorescent proteins to visualize cancer in vivo. *Nat. Rev. Cancer* **5**:796–806.
6. Umeoka, T., et al. 2004. Visualization of intrathoracically disseminated solid tumors in mice with optical imaging by telomerase-specific amplification of a transferred green fluorescent protein gene. *Cancer Res.* **64**:6259–6265.
7. Watanabe, T., et al. 2006. Histone deacetylase inhibitor FR901228 enhances the antitumor effect of telomerase-specific replication-selective adenoviral agent OBP-301 in human lung cancer cells. *Exp. Cell Res.* **312**:256–265.
8. Fujiwara, T., et al. 2006. Enhanced antitumor efficacy of telomerase-selective oncolytic adenoviral agent OBP-401 with docetaxel: Preclinical evaluation of chemovirotherapy. *Int. J. Cancer.* **119**:432–440.
9. Glinskii, A.B., et al. 2003. Viable circulating metastatic cells produced in orthotopic but not ectopic prostate cancer models. *Cancer Res.* **63**:4239–4243.
10. Kishimoto, H., et al. 2006. In vivo imaging of lymph node metastasis with telomerase-specific replication-selective adenovirus. *Nat. Med.* **12**:1213–1219.
11. Kawashima, T., et al. 2004. Telomerase-specific replication-selective virotherapy for human cancer. *Clin. Cancer Res.* **10**:285–292.
12. Taki, M., et al. 2005. Enhanced oncolysis by a tropism-modified telomerase-specific replication-selective adenoviral agent OBP-405 ('Telomelysin-RGD'). *Oncogene.* **24**:3130–3140.
13. Paterlini-Brechot, P., and Benali, N.L. 2007. Circulating tumor cells (CTC) detection: clinical impact and future directions. *Cancer Lett.* **253**:180–204.
14. Umetani, N., et al. 2006. Prediction of breast tumor progression by integrity of free circulating DNA in serum. *J. Clin. Oncol.* **24**:4270–4276.
15. Li, Y., et al. 2006. Serum circulating human mRNA profiling and its utility for oral cancer detection. *J. Clin. Oncol.* **24**:1754–1760.
16. Diehl, F., et al. 2008. Circulating mutant DNA to assess tumor dynamics. *Nat. Med.* **14**:985–990.
17. Allard, W.J., et al. 2004. Tumor cells circulate in the peripheral blood of all major carcinomas but not in healthy subjects or patients with nonmalignant diseases. *Clin. Cancer Res.* **10**:6897–6904.
18. Half, E., et al. 2004. HER-2 receptor expression, localization, and activation in colorectal cancer cell lines and human tumors. *Int. J. Cancer.* **108**:540–548.
19. Fehm, T., et al. 2002. Cytogenetic evidence that circulating epithelial cells in patients with carcinoma are malignant. *Clin. Cancer Res.* **8**:2073–2084.
20. Willipinski-Stapelfeldt, B., et al. 2005. Changes in cytoskeletal protein composition indicative of an epithelial-mesenchymal transition in human micrometastatic and primary breast carcinoma cells. *Clin. Cancer Res.* **11**:8006–8014.
21. Thiery, J.P. 2002. Epithelial-mesenchymal transitions in tumour progression. *Nat. Rev. Cancer.* **2**:442–454.
22. Yilmaz, M., and Christofori, G. 2009. EMT, the cytoskeleton, and cancer cell invasion. *Cancer Metastasis Rev.* **28**:15–33.
23. Rees, J.R., Onwuegbusi, B.A., Save, V.E., Alderson, D., and Fitzgerald, R.C. 2006. In vivo and in vitro evidence for transforming growth factor-beta1-mediated epithelial to mesenchymal transition in esophageal adenocarcinoma. *Cancer Res.* **66**:9583–9590.
24. Nagrath, S., et al. 2007. Isolation of rare circulating tumour cells in cancer patients by microchip technology. *Nature.* **450**:1235–1239.
25. Frederick, B.A., et al. 2007. Epithelial to mesenchymal transition predicts gefitinib resistance in cell lines of head and neck squamous cell carcinoma and non-small cell lung carcinoma. *Mol. Cancer Ther.* **6**:1683–1691.
26. Xi, L., et al. 2007. Optimal markers for real-time quantitative reverse transcription PCR detection of circulating tumor cells from melanoma, breast, colon, esophageal, head and neck, and lung cancers. *Clin. Chem.* **53**:1206–1215.
27. Ignatiadis, M., et al. 2008. Prognostic value of the molecular detection of circulating tumor cells using a multimarker reverse transcription-PCR assay for cytokeratin 19, mammaglobin A, and HER2 in early breast cancer. *Clin. Cancer Res.* **14**:2593–2600.
28. Blackburn, E.H. 2000. Telomere states and cell fates. *Nature.* **408**:53–56.
29. Santisteban, M., et al. 2009. Immune-induced epithelial to mesenchymal transition in vivo generates breast cancer stem cells. *Cancer Res.* **69**:2887–2895.
30. Dembinski, J.L., and Krauss, S. 2009. Characterization and functional analysis of a slow cycling stem cell-like subpopulation in pancreas adenocarcinoma. *Clin. Exp. Metastasis.* Online publication ahead of print. doi:10.1007/s10585-009-9260-0.
31. Maurelli, R., et al. 2006. Inactivation of p16INK4a (inhibitor of cyclin-dependent kinase 4A) immortalizes primary human keratinocytes by maintaining cells in the stem cell compartment. *FASEB J.* **20**:1516–1518.
32. Maida, Y., et al. 2009. Diagnostic potential and limitation of imaging cancer cells in cytological samples using telomerase-specific replicative adenovirus. *Int. J. Oncol.* **34**:1549–1556.
33. Wickham, T.J., Mathias, P., Cheresh, D.A., and Nemerow, G.R. 1993. Integrins alpha v beta 3 and alpha v beta 5 promote adenovirus internalization but not virus attachment. *Cell.* **73**:309–319.
34. Kawabata, K., Sakurai, F., Koizumi, N., Hayakawa, T., and Mizuguchi, H. 2006. Adenovirus vector-mediated gene transfer into stem cells. *Mol. Pharm.* **3**:95–103.
35. Scher, H.I., et al. 2009. Circulating tumour cells as prognostic markers in progressive, castration-resistant prostate cancer: a reanalysis of IMMC38 trial data. *Lancet Oncol.* **10**:233–239.